




High-sensitivity measurements of the nonlinear absorption coefficient of wide bandgap oxide thin films with the Z-scan method

MEILING CHEN,^{1,2,3} JIANDA SHAO,^{1,3,4,6} YUANAN ZHAO,^{1,3,7}
GUOHANG HU,^{1,3} MEIPING ZHU,^{1,3,4} YINGJIE CHAI,⁵  KAIXIN
ZHANG,^{1,2,3} AND HAO MA^{1,2,3}

¹Laboratory of Thin Film Optics, Shanghai Institute of Optics and Fine Mechanics, Chinese Academy of Sciences, Shanghai, 201800, China

²Center of Materials Science and Optoelectronics Engineering, University of Chinese Academy of Sciences, Beijing, 100049, China

³Key Laboratory of Materials for High Power Laser, Chinese Academy of Sciences, Shanghai, 201800, China

⁴Hangzhou Institute for Advanced Study, University of Chinese Academy of Sciences, Hangzhou, 310024, China

⁵CREOL, College of Optics and Photonics, University of Central Florida, Orlando, Florida, 32816, USA

⁶jdshao@siom.ac.cn

⁷yazhao@siom.ac.cn

Abstract: The nonlinear response of wide bandgap oxide thin films gradually emerges and attracts attention with the development of an ultra-short and ultra-intense laser. In Z-scan technique, due to the extremely lower nonlinear response of thin film compared with the common substrate, it isn't easy to measure the multiphoton absorption coefficient of wide bandgap oxide thin films. In this study, a method is proposed to suppress the substrate impact and improve the thin film measurement sensitivity. To make the thin film nonlinear intensity dominate the total intensity, including unwanted substrate impact, material and thickness of the substrate are analyzed. Considering the nonlinear effects of different substrates and the adhesion between the substrate and the thin film, 50 μm MgF_2 and quartz glass are selected as the substrate for deposition. The nonlinear intensity of substrate is suppressed to at least 80% of the whole element or can even be ignored so that the normalized transmittance of the thin film can be obtained effectively. The two-photon and three-photon absorption coefficients of HfO_2 , Al_2O_3 , and SiO_2 thin film are measured at different wavelengths. The nonlinear absorption response measurements of wide bandgap oxide thin films can advance the design and fabrication of low-loss photonic devices in ultra-fast lasers.

© 2022 Optica Publishing Group under the terms of the [Optica Open Access Publishing Agreement](#)

1. Introduction

Thin-film elements play an extremely important role in all kinds of laser systems. For example, high-reflective mirrors, anti-reflective mirrors, and polarizers are essential in the high-power laser systems. These thin-films are usually consisted of wide bandgap oxide materials with high laser damage threshold and mature deposition technologies [1–3], such as HfO_2 and SiO_2 , as the high and low refractive index material [4,5]. With the development of ultra-short and ultra-intense laser, the optical nonlinear effects in films cannot be ignored, such as nonlinear absorption [6,7], Kerr effect [8,9], and frequency conversion [10,11]. From the perspective of output laser, these effects are harmful to the pulse quality and need to be restrained. In Ref. [7], due to the two-photon absorption of the dielectric multilayer, the high reflection performance of the mirror was seriously affected. On the other hand, the exploitation of the nonlinear effect in films is desirable. It was predicated that multilayer structure composed of wide bandgap

oxide material could achieve a triple frequency conversion efficiencies larger than ten percent [12]. It is important to determine the optical nonlinear coefficient of wideband oxide layers for manipulating the optical nonlinear performance.

The Z-scan technique [13–20] is widely used to measure optical nonlinearity of the material because of its efficiency and convenience. The nonlinear properties of the thin film are quite different from the bulk, especially as for the wide bandgap oxide materials. The thin film is fabricated on the substrate with a similar optical bandgap and a thickness that is thousands of times larger. There are challenges to obtain the film's nonlinear response, due to extracting it from the total Z-scan intensity including unwanted contribution of the substrate. In previous work, the nonlinear absorption coefficient of the thin metal films [15], semiconductor films [17,18], etc., which were prepared on the quartz or BK7 with millimeter thickness, were measured by the Z-scan method. These films with narrow or zero optical bandgap showed a much larger nonlinear response than the substrate material, so there is no need to consider the substrate. In 2019, T. R. Ensley, S. Benis *et al.* proposed dual-arm Z-scan method when the substrate background signal is large during the measurement [19]. By scanning the thin film sample and the bare in two laser beams simultaneously, the substrate effect can be correctly eliminated if the Z-Position between two arms are completely identical. As for the wide bandgap oxide thin film, its nonlinear response is very weak. Suppressing the nonlinear response of the substrate is one of the key to improve the measurement ability. The former method of dual-arm Z-scan is efficient, but increases the difficulty of operating in matching two arms. Highly suppressing the nonlinear response of the substrate by regulating the substrate material and thickness is another way to obtain the thin film nonlinear response efficiently, and has the advantages of simplicity and high-sensitivity.

In this paper, 50 μm MgF_2 and quartz glass are selected as the substrate to prepared wide bandgap oxide thin films. Due to the efficient suppression of the unwanted substrate impacts during Z-scan measurement, the normalized transmittance of thin films can be obtained directly with ignorance of substrate or extracted from the whole sample effectively. To verify the better performance of the wider bandgap and thinner thickness substrate, the two-photon absorption (2PA) and three-photon absorption (3PA) coefficient of HfO_2 , Al_2O_3 , and SiO_2 thin film are measured at laser wavelengths of 343 nm and 515 nm with 1 kHz repetition rate. The measurement results are important for their application in high-power laser.

2. Theories and experiment

2.1. Two-photon absorption (2PA) and three-photon absorption (3PA)

Two-photon absorption (2PA) and three-photon absorption (3PA) are nonlinear absorption processes that can be regarded as electronic transitions from the valence band to the conduction band via one and two intermediate virtual states respectively. In an optical absorption process, the irradiance-dependent optical absorption coefficient $\alpha(I)$ can be written as:

$$\alpha(I) = \alpha_0 + \beta_2 I + \beta_3 I^2, \quad (1)$$

where I is the irradiation intensity; α_0 is the linear absorption coefficient; β_2 and β_3 represent 2PA and 3PA coefficient, respectively. The 2PA and 3PA process occurs when the material bandgap E_g and excitation photon energy E_p satisfy $E_p < E_g < 2E_p$ and $2E_p < E_g < 3E_p$, respectively. In our experiment, the photon energy is 3.6 eV (343 nm) and 2.4 eV (515 nm). The optical bandgap E_g of the materials is shown in Table 1. Based on the comparison of material bandgap and the energy of two (and three) photons, it is believed that HfO_2 and Al_2O_3 both mainly perform 2PA at 343 nm and 3PA at 515 nm, and SiO_2 mainly shows 3PA response in 343 nm.

2.2. Z-Scan measurement

The experimental setup diagram is shown in Fig. 1. The setup consists of a femtosecond laser (Light Conversion, CB5-05) with wavelength of 1030 nm, which pumps a harmonic module

Table 1. Optical bandgap E_g of HfO_2 , Al_2O_3 , and SiO_2 thin film

Material	Bandgap E_g (eV)	References
HfO_2	5.4~5.8	[21–24]
Al_2O_3	6.2~7.1	[25, 26, 27]
SiO_2	8.3~9.7	[25, 27, 28]

(Light Conversion, 2H-3H) and produces pulses in the wavelengths of 515 nm and 343 nm with ~ 300 fs and ~ 200 fs pulse width (FWHM) respectively, providing excitation sources for our experiment. In our experiment, the laser is operated at 1 KHz repetition rate. According to the related research in Ref. [29–31], this rate is not enough to produce the thermal lens effect. An attenuator composed of a half-wave plate and a polarizer is used to change the irradiation energy. An expander makes the laser diameter ~ 4 mm (measured by a beam quality analyzer, Coherent). Two beams of laser are obtained by a beam splitter and focused by the lens with the focal length of 150 mm. The waist radius of the focused beams are about $8 \mu\text{m}$ and $12 \mu\text{m}$ in the wavelengths of 343 nm and 515 nm, respectively. The sample is placed on a mobile platform controlled by a computer and moves along the optical axis (Z axis). The transmittance data are collected by two power meters (Ophir).

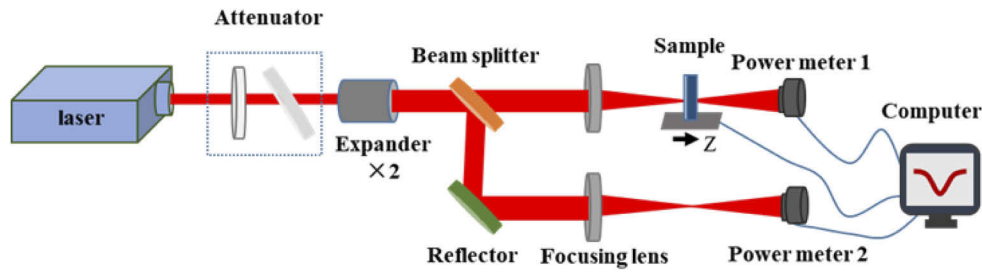


Fig. 1. The Z-Scan setup diagram.

The spectrum (detected by a spectrometer, Ocean Optics) of the laser in front or behind the sample shows no different or shift during scanning. It is regarded that the self-phase modulation (SPM) and the white-light continua aren't induced in our experiment. According to the Ref. [32,33], influence of group velocity dispersion (GVD) is very weak and can be negligible.

The traditional models are applied to describe the relations between the normalized transmittance and the 2PA coefficient β_2 and 3PA coefficient β_3 , which is described as [14,34]:

$$T_{2PA}(z) = \sum_{m=0}^{\infty} \frac{(-q(0, z))^m}{(m+1)^{3/2}}, \quad q(0, z) = \frac{\beta_2 L_{eff} I_{00}}{1 + z^2/z_0^2} \quad (2)$$

and

$$T_{3PA}(z) = \sum_{m=0}^{\infty} \frac{(-p(0, z))^m}{(2m+1)!(2m+1)^{1/2}}, \quad p(0, z) = \frac{2\beta_3 L'_{eff} I_{00}^2}{(1 + z^2/z_0^2)^2}, \quad (3)$$

where T_{2PA} and T_{3PA} represent the normalized transmittance in the process of 2PA and 3PA respectively; $z_0 = \pi\omega_0^2/\lambda$ is Rayleigh length; $L_{eff} = (1 - e^{-\alpha_0 L})/\alpha_0$ and $L'_{eff} = (1 - e^{-2\alpha_0 L})/2\alpha_0$ are the effective thickness of 2PA and 3PA response respectively; $\alpha_0 = 4\pi\kappa/\lambda$ is the linear absorption coefficient of the sample, and κ represent the extinction coefficient that is measured by an ellipsometer (Horiba UVISEL-2) in our study; I_{00} is laser peak intensity at the focus point; β_2 and β_3 are 2PA and 3PA coefficient respectively; λ , ω_0 and L are laser wavelength, waist radius

at the focal point, and physical thickness of the sample respectively. Using this model, β_2 and β_3 can be extracted from the results by finding a best fitting curve of the normalized transmittance data obtained from Z-scan measurement.

2.3. Thin-film material preparation

The HfO_2 , Al_2O_3 , and SiO_2 thin film are fabricated by electron beam evaporation (EBE) technique. The borosilicate glass (18 mm×18 mm×0.17 mm), quartz glass ($\Phi 10$ mm×50 μm), and MgF_2 ($\Phi 10$ mm×50 μm) are used as the substrate to prepare the thin film. During the deposition process, the substrate temperature is 25 °C. The base pressure is $\sim 2 \times 10^{-3}$ Pa. The deposition rate is 0.1 nm/s for HfO_2 film, 0.8 nm/s for Al_2O_3 film and 0.3 nm/s for SiO_2 film respectively.

2.4. Selection of substrate

Initially, the borosilicate glass with thickness of 0.17 mm is used as the substrate for preparing wide bandgap oxide thin-films. As shown in Fig. 2(a), during the open aperture (OA) Z-scan measurement, the normalized transmittance signal of the film sample is almost overlapped with the bare substrate. The nonlinear response of the thin film cannot be measured because of the huge contribution from the substrate. To suppress the substrate impact, the material and thickness of the substrate are analyzed. In Ref. [35], it is reported that the MgF_2 bulk shows no nonlinear response at 355 nm or 266 nm. According to Eq. (3) ~ Eq. (6), the thicker sample will produce a stronger nonlinear response, so the thickness of the substrate is important for the thin film measurement. Fig. 2(b) shows the normalized transmittance measured by OA Z-scan when different substrates move along the optical axis. The intensity fluctuations of 50 μm MgF_2 (blue), 0.1 mm MgF_2 (purple), 50 μm CaF_2 (yellow) and 50 μm quartz glass (green) are 0.38%, 0.49%, 0.68% and 0.89% respectively. It can be concluded that even under high-intensity laser irradiation, 50 μm MgF_2 appears minimal nonlinear response and can be selected for preparing wide bandgap oxide thin films. Particularly, as for SiO_2 thin film, considering the poor adhesion between SiO_2 film and fluoride substrate, it is prepared on the 50 μm quartz glass substrate.

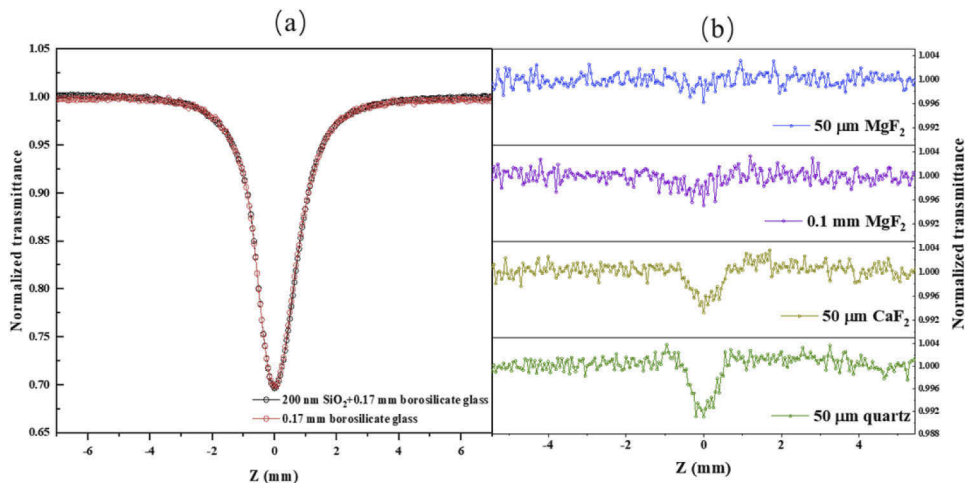


Fig. 2. At laser wavelength of 515 nm, (a) the normalized transmittances of 200 nm SiO_2 plus 0.17 mm borosilicate glass (black) and the bare 0.17 mm borosilicate glass (red) measured in OA Z-scan at 1.6 μJ input; (b) the normalized transmittances of 50 μm MgF_2 (blue), 0.1 mm MgF_2 (purple), 50 μm CaF_2 (yellow), and 50 μm quartz glass (green) measured by OA Z-Scan at 2 μJ input.

2.5. Acquisition of thin-film nonlinear absorption signal

To determine the nonlinear absorption, the thin film element and the bare substrate are measured by two sequential OA Z-scans. Although the nonlinear response of the thin film is weak, the substrate impact is greatly suppressed or even can be ignored. As can be seen from Fig. 3(a), compared to the nonlinear transmittance of the whole thin film sample (T_{f+s}), the bare substrate (T_s) has little nonlinear response, so there is no need to consider the substrate impact. The signal T_{f+s} can represent the nonlinear response of the thin film directly. In Fig. 3(b), the nonlinear response of the bare substrate (T_s) occupies a proportion in the total intensity (T_{f+s}). The normalized transmittance of thin film needs to be extracted. In our experiment, the influence of Fresnel reflections and low finesses cavities are ignored. We regard that the optical nonlinear response intensity of the thin film with the substrate is the sum of the thin film and the bare substrate. The normalized transmittance of the thin-film T_f can be extracted as:

$$T_f = 1 + (T_{f+s} - T_s). \quad (4)$$

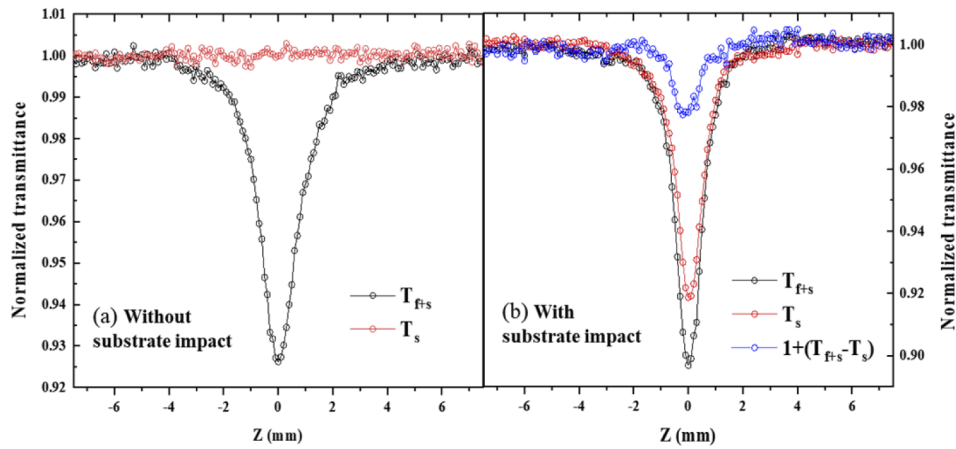


Fig. 3. The normalized transmittances measured by OA Z-Scan at $\lambda=343$ nm of (a) 623 nm HfO_2 with 50 μm MgF_2 (T_{f+s} , black dotted line) and bare 50 μm MgF_2 (T_s , red dotted line) at 0.6 μJ ; (b) 700 nm SiO_2 with 50 μm quartz glass (T_{f+s} , black dotted line), bare 50 μm quartz glass (T_s , red dotted line) and SiO_2 thin film extracted by $1+(T_{f+s}-T_s)$ (blue dotted line) at 1.6 μJ .

3. Results and discussion

3.1. Measurement result of HfO_2 thin film with 50 μm MgF_2 substrate at 343 nm and 515 nm

As for 623 nm HfO_2 thin film with 50 μm MgF_2 substrate, it can be concluded from Fig. 4 that the 50 μm MgF_2 shows no nonlinear response at $\lambda=343$ nm with laser intensities $I_1 = 1.45 \times 10^3$ GW/cm^2 and $\lambda=515$ nm with laser intensities $I_2 = 3.90 \times 10^3$ GW/cm^2 . The substrate impact can be ignored when the laser peak intensity at focus point $I_{00} \leq I_1$ at $\lambda=343$ nm (or $\leq I_2$ at $\lambda=515$ nm) during Z-scan measurement. The measured data and best fitting with a laser intensity of 0.71×10^3 $\text{GW}/\text{cm}^2 \sim 1.45 \times 10^3$ GW/cm^2 at $\lambda=343$ nm are shown in Fig. 5(a), and 3.21×10^3 $\text{GW}/\text{cm}^2 \sim 3.90 \times 10^3$ GW/cm^2 at $\lambda=515$ nm are shown in Fig. 5(b). The corresponding 2PA coefficient (β_2) and 3PA coefficient (β_3) of HfO_2 thin film are listed in Table 2.

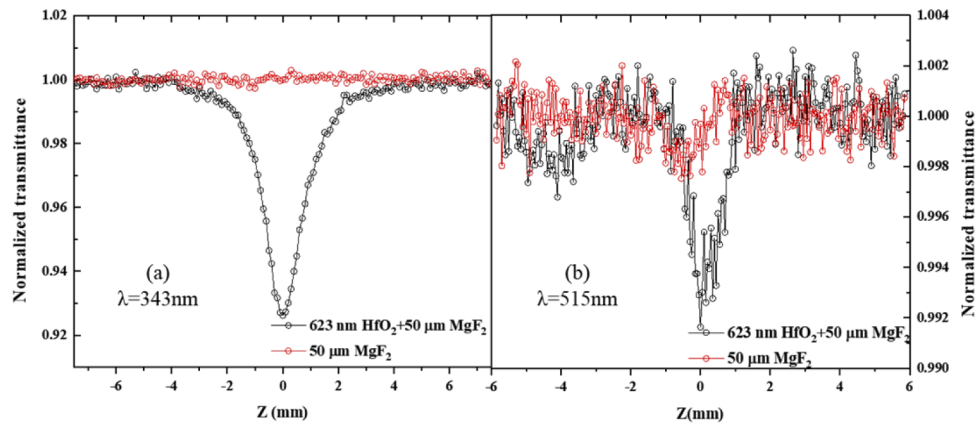


Fig. 4. The normalized transmittance of 623 nm HfO_2 with 50 $\mu\text{m MgF}_2$ substrate (black dotted line) and the bare 50 $\mu\text{m MgF}_2$ (red dotted line) at (a) $\lambda = 343 \text{ nm}$ with laser intensities of $1.45 \times 10^3 \text{ GW/cm}^2$ and (b) $\lambda = 515 \text{ nm}$ with laser intensities of $3.90 \times 10^3 \text{ GW/cm}^2$ respectively.

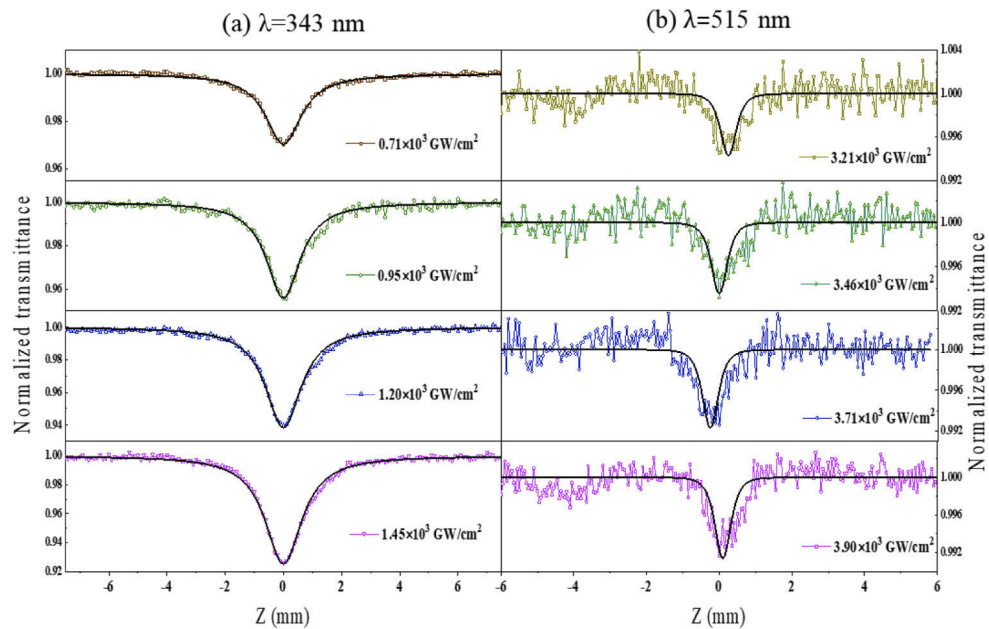


Fig. 5. Experimental data (dotted line) and fitting curve (solid line) of 623 nm HfO_2 thin film at (a) $\lambda = 343 \text{ nm}$ with laser intensities of $0.71 \times 10^3 \text{ GW/cm}^2$, $0.95 \times 10^3 \text{ GW/cm}^2$, $1.20 \times 10^3 \text{ GW/cm}^2$, $1.45 \times 10^3 \text{ GW/cm}^2$ and (b) $\lambda = 515 \text{ nm}$ with laser intensities of $3.21 \times 10^3 \text{ GW/cm}^2$, $3.46 \times 10^3 \text{ GW/cm}^2$, $3.71 \times 10^3 \text{ GW/cm}^2$, $3.90 \times 10^3 \text{ GW/cm}^2$ respectively.

Table 2. Laser intensity I_{00} and corresponding 2PA and 3PA coefficient for HfO_2 thin film at 343 nm and 515 nm, respectively.

$\text{HfO}_2, \lambda=343 \text{ nm}$ (2PA response)				
I_{00} (GW/cm ²)	0.71×10^3	0.95×10^3	1.20×10^3	1.45×10^3
β_2 (cm/GW)	1.95	2.06	2.34	2.39
$\text{HfO}_2, \lambda=515 \text{ nm}$ (3PA response)				
I_{00} (GW/cm ²)	3.21×10^3	3.46×10^3	3.71×10^3	3.90×10^3
β_3 (cm ³ /GW ³)	5.05×10^{-5}	4.93×10^{-5}	5.13×10^{-5}	5.11×10^{-5}

3.2. Measurement result of Al_2O_3 thin film with $50 \mu\text{m}$ MgF_2 substrate at 343 nm and 515 nm

The 200 nm Al_2O_3 thin film is deposited on the $50 \mu\text{m}$ MgF_2 substrate. Figure 6(a) shows that at $\lambda=343 \text{ nm}$ with laser intensity $I_1 = 962 \text{ GW/cm}^2$, the substrate performs no nonlinear response (red dotted line). When the laser intensity $I_{00} \leq I_1$, the substrate impact can be ignored and the nonlinear response of the film are easily obtained. With $I_{00} = 552 \text{ GW/cm}^2 \sim 962 \text{ GW/cm}^2$, the normalized transmittances of 200 nm Al_2O_3 (dotted line) and fitting curves based on 2PA theory (solid line) are shown in Fig. 7(a). As can be seen from Fig. 6(b), at irradiation wavelength of 515 nm with intensity $I_2 = 4.67 \times 10^3 \text{ GW/cm}^2$, the nonlinear signal of $50 \mu\text{m}$ MgF_2 occupies $\sim 20\%$ of the total signal. Due to the existence of the substrate impact (red dotted line), the normalized transmittance of thin film (blue dotted line) needs to be extracted from the total signal (black dotted line). Under different intensities within $3.73 \times 10^3 \text{ GW/cm}^2 \sim 4.67 \times 10^3 \text{ GW/cm}^2$ ($\leq I_2$), the extraction results (dotted line) and best fitting based on 3PA theory (solid line) are shown in Fig. 7(b). Table 3 lists corresponding 2PA and 3PA coefficients.

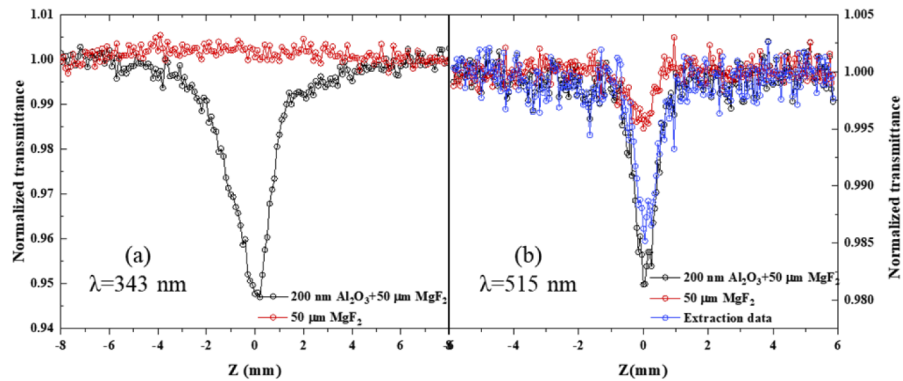


Fig. 6. The normalized transmittance of 200 nm Al_2O_3 with $50 \mu\text{m}$ MgF_2 substrate (black dotted line) and the bare $50 \mu\text{m}$ MgF_2 (red dotted line) at (a) $\lambda=343 \text{ nm}$ with intensity of 962 GW/cm^2 and (b) $\lambda=515 \text{ nm}$ with intensity of $4.67 \times 10^3 \text{ GW/cm}^2$ respectively. The extraction data in (b) represent the normalized transmittance of the Al_2O_3 thin film (blue dotted line).

3.3. Measurement result of SiO_2 thin film with $50 \mu\text{m}$ quartz glass substrate at 343 nm

As for 700 nm SiO_2 thin film fabricated on $50 \mu\text{m}$ quartz glass, at an irradiation wavelength of 343 nm with intensity of $5.55 \times 10^3 \text{ GW/cm}^2$, compared with the nonlinear response of the whole thin film element (Fig. 8(a), black dotted line), the substrate cannot be ignored (Fig. 8(a), red dotted line). The extracting process of the thin film normalized transmittance is made, and the result shows that it occupies about 20% of the total intensity (Fig. 8(a), blue dotted line). With

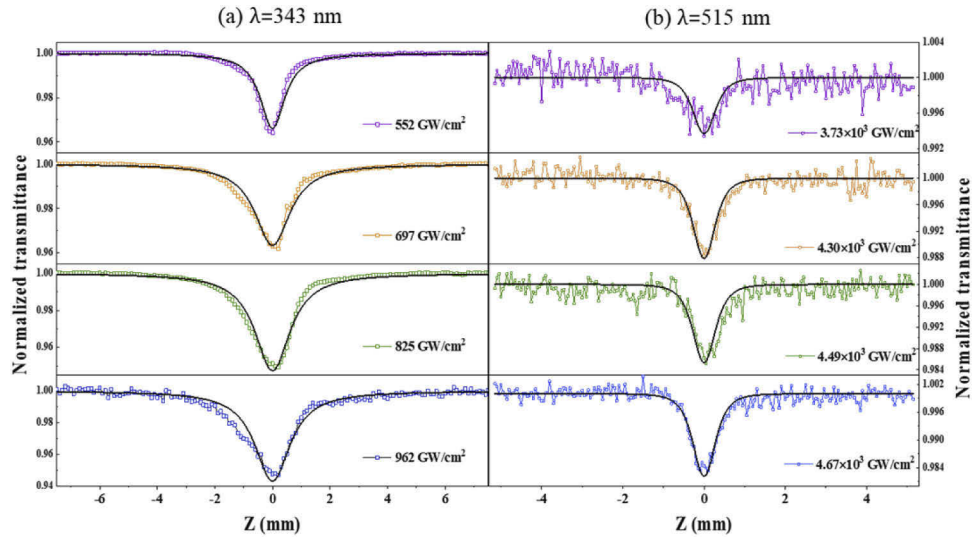


Fig. 7. Experimental data (dotted line) and fitting curve (black solid line) of 200 nm Al_2O_3 thin film at (a) $\lambda=343$ nm with laser intensities of 552 GW/cm^2 , 697 GW/cm^2 , 825 GW/cm^2 , 962 GW/cm^2 and (b) $\lambda=515$ nm with laser intensities of 3.73×10^3 GW/cm^2 , 4.30×10^3 GW/cm^2 , 4.49×10^3 GW/cm^2 , 4.67×10^3 GW/cm^2 respectively.

Table 3. Laser intensity I_{00} and corresponding 2PA and 3PA coefficient for Al_2O_3 thin film at 343 nm and 515 nm, respectively.

Al_2O_3 , $\lambda=343$ nm (2PA response)				
I_{00} (GW/cm^2)	552	697	825	962
β_2 (cm/GW)	7.24	7.58	9.17	8.5
Al_2O_3 , $\lambda=515$ nm (3PA response)				
I_{00} (GW/cm^2)	3.73×10^3	4.30×10^3	4.49×10^3	4.67×10^3
β_3 (cm^3/GW^3)	0.74×10^{-4}	2.34×10^{-4}	1.94×10^{-4}	2.17×10^{-4}

different irradiation intensity, the normalized transmittance of SiO_2 thin film (dotted line) and those best fitting with 3PA theory (solid line) are shown in Fig. 8(b). The corresponding 3PA coefficients during the fitting process with a laser intensity of 3.81×10^3 $\text{GW}/\text{cm}^2 \sim 5.55 \times 10^3$ GW/cm^2 are listed in Table 4.

Table 4. Laser intensity I_{00} and corresponding 3PA coefficient for SiO_2 thin film at 343 nm.

SiO_2 thin film, $\lambda=343$ nm (3PA response)				
I_{00} (GW/cm^2)	3.81×10^3	4.52×10^3	4.92×10^3	5.55×10^3
β_3 (cm^3/GW^3)	9.15×10^{-5}	9.57×10^{-5}	8.81×10^{-5}	8.47×10^{-5}

3.4. Measurement result of Al_2O_3 and SiO_2 bulk material

In addition to the thin film materials above, the nonlinear absorption response of Al_2O_3 bulk (sapphire window) with 0.5 mm thickness and SiO_2 material (quartz glass) with 0.5 mm and 50 μm thickness are measured. The 2PA and 3PA coefficient of sapphire is measured to be $2.4 \times 10^{-3} \sim 7.1 \times 10^{-3}$ cm/GW and $2.03 \times 10^{-6} \sim 5.01 \times 10^{-6}$ cm^3/GW^2 at laser wavelength of 343 nm and 515 nm, respectively. Their normalized transmittance and best fitting under different

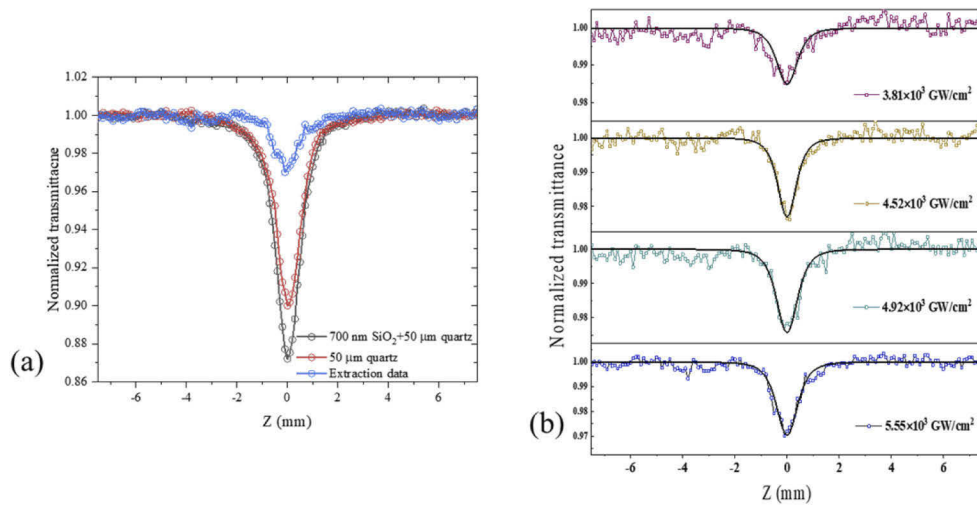


Fig. 8. (a) The normalized transmittance of 700 nm SiO₂ with 50 μm quartz glass (black dotted line), the bare 50 μm quartz glass (red dotted line) and extraction data (blue dotted line) at $\lambda=343$ nm with intensity of 5.55×10^3 GW/cm². (b) The normalized transmittance of 700 nm SiO₂ thin film extracted (dotted line) and best fitting (solid line) with laser intensities of 3.81×10^3 GW/cm², 4.52×10^3 GW/cm², 4.92×10^3 GW/cm² and 5.55×10^3 GW/cm² respectively.

irradiation energy are shown in Fig. 9 (a) and (b). As for the quartz glass, the excitation energy required for 50 μm bulk is greater than 0.5 mm bulk. 3PA theory is used to fitting the measured data of quartz glass at 343 nm, as shown in Fig. 9(c) and (d). 3PA coefficient of $4.76 \times 10^{-6} \sim 9.29 \times 10^{-6}$ cm³/GW² and $2.59 \times 10^{-6} \sim 2.77 \times 10^{-6}$ cm³/GW² are extracted with different laser energy for 0.5 mm and 50 μm quartz glass, respectively.

3.5. Discussion

In our work, through regulating the substrate material and thickness, the nonlinear signal of the thin film is dominant in the total nonlinear signal of the whole sample. The proportions of the thin film are both $\sim 100\%$ for HfO₂ at 343 nm and 515 nm, $\sim 100\%$ for Al₂O₃ at 515 nm, $\sim 80\%$ for Al₂O₃ at 343 nm, and $\sim 20\%$ for SiO₂ at 343 nm. Based on the above, the nonlinear absorption coefficients of the thin film are measured with high sensitivity. All measurement results of the wide bandgap thin film and corresponding bulk materials are listed in Table 5. The uncertainties in β_2 and β_3 mainly originate from the determination of the irradiance distribution (for example, beam waist and pulse width) during the measurement. The 2PA coefficients are measured to be $2.19 \pm 11\%$ cm/GW for HfO₂ thin film and $8.12 \pm 13\%$ cm/GW for Al₂O₃ thin film at 343 nm, respectively. The 3PA coefficients are measured to be $5.00 \times 10^{-5} \pm 3\%$ cm³/GW² for HfO₂ thin film at 515 nm, $1.80 \times 10^{-4} \pm 59\%$ cm³/GW² Al₂O₃ thin film at 515 nm, and $9.00 \times 10^{-5} \pm 6\%$ cm³/GW² for SiO₂ thin film at 343 nm. The 2PA coefficient of crystalline sapphire was reported in Ref. [35] and Ref. [36] at laser wavelength of 264 nm and 266 nm, respectively. We note that their result $\sim 9 \times 10^{-2}$ cm/GW is larger than our result at 343 nm for sapphire window glass with 4.50×10^{-3} cm/GW, which is possibly caused by laser wavelength change or the sample difference. From Table 5, it is can be seen that the β_2 value of Al₂O₃ thin film is 1000 times larger than that of sapphire window. The β_3 value of Al₂O₃ and SiO₂ thin film are dozens of times that of their bulk state. This phenomenon that shows the big nonlinear coefficient difference between the film and the bulk also appears in other materials, such as ZnSe (film in Ref. [37] and bulk in Ref. [38]) and ZnO (film in Ref. [39] and bulk in Ref. [40]).

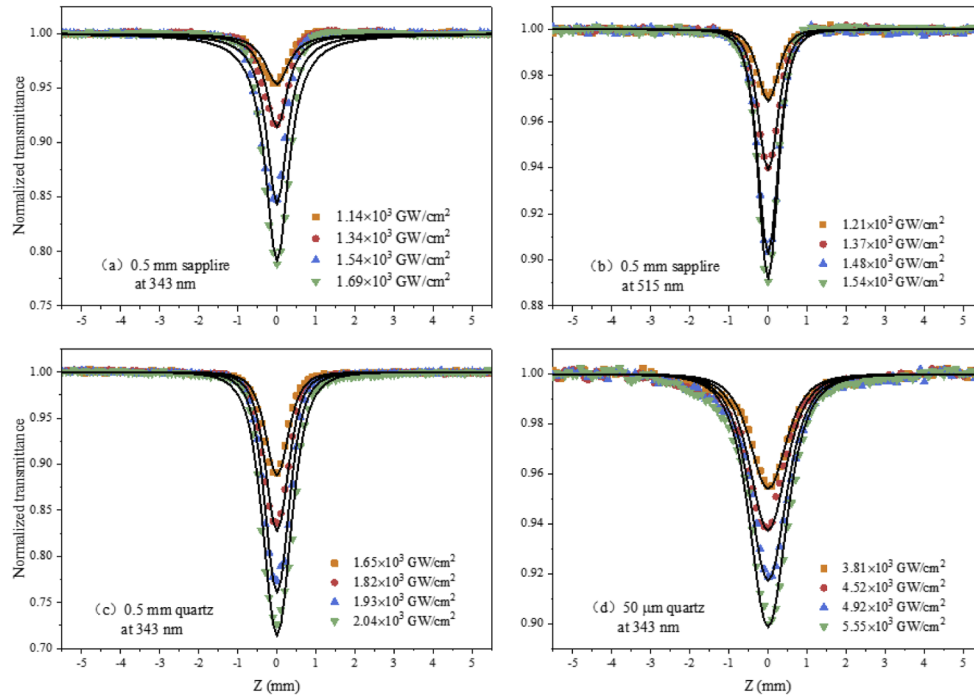


Fig. 9. The measured data (dots) and best fitting (solid line) under different irradiation energy of (a) 0.5 mm sapphire at 343 nm with 2PA theory, (b) 0.5 mm sapphire at 515 nm with 3PA theory, (c) 0.5 mm and (d) 50 μm quartz glass at 343 nm with 3PA theory.

Table 5. 2PA and 3PA experimental result for HfO_2 , SiO_2 , and Al_2O_3 thin film or bulk materials

Material	state	Thickness	β_2 (cm/GW)	β_3 (cm ³ /GW ²)
HfO_2	thin film	623 nm	$2.19 \pm 11\%$ (at 343 nm)	$5.06 \times 10^{-5} \pm 3\%$ (at 515 nm)
Al_2O_3	thin film	200 nm	$8.12 \pm 13\%$ (at 343 nm)	$1.80 \times 10^{-4} \pm 59\%$ (at 515 nm)
SiO_2	thin film	700 nm	—	$9.00 \times 10^{-5} \pm 6\%$ (at 343 nm)
Al_2O_3	bulk (sapphire window)	0.5 mm	$4.50 \times 10^{-3} \pm 57\%$ (at 343 nm)	$3.87 \times 10^{-6} \pm 48\%$ (at 515 nm)
SiO_2	bulk (quartz glass)	50 μm	—	$2.71 \times 10^{-6} \pm 4\%$ (at 343 nm)
SiO_2	bulk (quartz glass)	0.5 mm	—	$7.04 \times 10^{-6} \pm 32\%$ (at 343 nm)

4. Conclusion

The method is proposed that the ultra-low nonlinear response and ultra-thin substrate is applied to prepare the wide bandgap oxide thin film. 50 μm MgF_2 and quartz glass are selected as substrates for preparing thin films. The unwanted nonlinear intensity contributed from the substrate is considerably suppressed or even can be ignored during the Z-Scan technique, which makes high sensitivity for identifying the multiphoton absorption coefficients of the thin film material. Using this method, the nonlinear absorption response of HfO_2 , Al_2O_3 and SiO_2 thin film are measured at laser wavelengths of 343 nm and 515 nm. By comparison with the corresponding bulk materials, it is found that the nonlinear coefficient of the thin film is much larger than that of the bulk. We believe the results in this paper to be the first measurement of the 2PA and 3PA coefficient of wide bandgap oxide monolayer film. Our work provides a highly sensitive method for the nonlinear optical parameter measurement of low-nonlinear-response oxide thin film, which is significant for manipulating the nonlinear performance of optical mirrors in ultra-fast lasers. In the future, other oxide thin film with wide band gap (such as Ta_2O_5 and Nb_2O_5) will be measured, and more different substrates will be analyzed.

Funding. National Key Research and Development Program of China (2018YFE0115900); National Natural Science Foundation of China (11874369, 52002271, U1831211); Strategic Priority Research Program of the Chinese Academy of Sciences (XDB1603), CAS special research assistant project.

Acknowledgments. This work was supported by the National Key R&D Program of China (Grant No. 2018YFE0115900), National Natural Science Foundation of China (Grant No. 11874369, U1831211 and 52002271), and Strategic Priority Research Program of the Chinese Academy of Sciences (Grant No. XDB1603), CAS special research assistant project.

Disclosures. The authors declare no conflicts of interest.

Data availability. Data underlying the results presented in this paper are not publicly available at this time but may be obtained from the authors upon reasonable request.

References

1. Q. Zhang, F. Pan, J. Luo, Q. Wu, Z. Wang, and Y. Wei, "Optical and laser damage properties of $\text{HfO}_2/\text{Al}_2\text{O}_3$ thin films deposited by atomic layer deposition," *J. Alloys Compd.* **659**, 288–294 (2016).
2. Z. Liu, Y. Zheng, F. Pan, Q. Lin, P. Ma, and J. Wang, "Investigation of laser induced damage threshold measurement with single-shot on thin films," *Appl. Surf. Sci.* **382**, 294–301 (2016).
3. B. Wang and L. Gallais, "A theoretical investigation of the laser damage threshold of metal multi-dielectric mirrors for high power ultrashort applications," *Opt. Express* **21**(12), 14698 (2013).
4. M. Li, L. Dong, L. Zhang, B. Wu, and J. Ma, "Design and fabrication of visible and infrared laser HR coating," *7th Int. Symp. Adv. Opt. Manuf. Test. Technol. Adv. Opt. Manuf. Technol.* 9281, 928128 (2014).
5. M. Zhan, W. Gao, T. Tan, H. He, J. Shao, and Z. Fan, "Study of $\text{Al}_2\text{O}_3/\text{MgF}_2$ HR coatings at 355 nm," *Vacuum* **79**(1-2), 90–93 (2005).
6. D. Faccio, M. Clerici, A. Averchi, O. Jedrkiewicz, S. Tzortzakis, D. Papazoglou, F. Bragheri, L. Tartara, A. Trita, S. Henin, I. Cristiani, A. Couairon, and P. Di Trapani, "Kerr-induced spontaneous Bessel beam formation in the regime of strong two-photon absorption," *Opt. Express* **16**(11), 8213 (2008).
7. O. Razskazovskaya, T. T. Luu, M. Trubetskov, E. Goulielmakis, and V. Pervak, "Nonlinear absorbance in dielectric multilayers," *Optica* **2**(9), 803 (2015).
8. E. Fedulova, M. Trubetskov, T. Amotchkina, K. Fritsch, P. Baum, O. Pronin, and V. Pervak, "Kerr effect in multilayer dielectric coatings," *Opt. Express* **24**(19), 21802 (2016).
9. T. Amotchkina, M. Trubetskov, and V. Pervak, "Experimental and numerical study of the nonlinear response of optical multilayers," *Opt. Express* **25**(11), 12675 (2017).
10. C. Rodríguez and W. Rudolph, "Modeling third-harmonic generation from layered materials using nonlinear optical matrices," *Opt. Express* **22**(21), 25984 (2014).
11. C. Rodríguez, S. Günster, D. Ristau, and W. Rudolph, "Frequency tripling mirror," *Opt. Express* **23**(24), 31594 (2015).
12. C. Rodríguez and W. Rudolph, "Modeling third harmonic generation from layered materials using nonlinear optical matrices: erratum," *Opt. Express* **23**(20), 26670 (2015).
13. A. A. Said and E. W. Van Stryland, "High-sensitivity, single-beam n 2 measurements," *Opt. Lett.* **14**, 955–957 (1989).
14. M. Sheik-Bahae, A. A. Said, T. H. Wei, D. J. Hagan, and E. W. Van Stryland, "Sensitive measurement of optical nonlinearities using a single beam," *IEEE J. Quantum Electron.* **26**(4), 760–769 (1990).
15. D. D. Smith, Y. Yoon, R. W. Boyd, J. K. Campbell, L. A. Baker, R. M. Crooks, and M. George, "Z-scan measurement of the nonlinear absorption of a thin gold film," *J. Appl. Phys.* **86**(11), 6200–6205 (1999).

16. F. Wang, S. Xu, Y. Feng, Y. Li, X. Zhang, Y. Xu, and J. Wang, "Characteristics of saturable absorption of MoS₂ films in the visible to near-infrared range," *Asia Commun. Photonics Conf. ACPC* **1**, AT11G.2 (2014).
17. Y. Xu, Y. Lu, Y. Zuo, F. Xu, and D. Zuo, "Z-scan measurements of nonlinear refraction and absorption for aluminum-doped zinc oxide thin film," *Appl. Opt.* **58**(22), 6112 (2019).
18. R. A. Ganeev, A. I. Rysanyansky, M. K. Kodirov, and T. Usmanov, "Two-photon absorption and nonlinear refraction of amorphous chalcogenide films," *J. Opt. A: Pure Appl. Opt.* **4**(4), 446–451 (2002).
19. T. R. Ensley, S. Benis, H. Hu, Z. Li, S.-H. Jang, A. K.-Y. Jen, J. W. Perry, J. M. Hales, D. J. Hagan, and E. W. Van Stryland, "Nonlinear refraction and absorption measurements of thin films by the dual-arm Z-scan method," *Appl. Opt.* **58**(13), D28 (2019).
20. H. Ma, Y. Zhao, Y. Shao, Y. Lian, W. Zhang, G. Hu, Y. Leng, and J. Shao, "Principles to tailor the saturable and reverse saturable absorption of epsilon-near-zero material," *Photonics Res.* **9**(5), 678 (2021).
21. M. C. Cheynet, S. Pokrant, F. D. Tichelaar, and J. L. Rouvire, "Crystal structure and band gap determination of HfO₂ thin films," *J. Appl. Phys.* **101**(5), 054101 (2007).
22. M. Kumar, R. P. Singh, and A. Kumar, "Opto-electronic properties of HfO₂: a first principle-based spin-polarized calculations," *Optik*. **226**, 165937 (2021).
23. F. L. Martínez, M. Toledano-Luque, J. J. Gandía, J. Cárabe, W. Bohne, J. Röhrich, E. Strub, and I. Mártil, "Optical properties and structure of HfO₂ thin films grown by high pressure reactive sputtering," *J. Phys. D: Appl. Phys.* **40**(17), 5256–5265 (2007).
24. W. Deng, C. Jin, C. Li, S. Yao, B. Yu, and Y. Liu, "Plasma-ion-assisted deposition of HfO₂ films with low UV absorption," *Surf. Coatings Technol.* **395**, 125691 (2020).
25. C. Rodríguez and W. Rudolph, "Characterization and $\chi^{(3)}$ measurements of thin films by third-harmonic microscopy," *Opt. Lett.* **39**(20), 6042 (2014).
26. M. L. Huang, Y. C. Chang, C. H. Chang, T. D. Lin, J. Kwo, T. B. Wu, and M. Hong, "Energy-band parameters of atomic-layer-deposition Al₂O₃/InGaAs heterostructure," *Appl. Phys. Lett.* **89**, 2006–2008 (2006).
27. D. Tahir, H. L. Kwon, H. C. Shin, S. K. Oh, H. J. Kang, S. Heo, J. G. Chung, J. C. Lee, and S. Tougaard, "Electronic and optical properties of Al₂O₃/SiO₂ thin films grown on Si substrate," *J. Phys. D: Appl. Phys.* **43**(25), 255301 (2010).
28. E. Güler, G. Uğur, Uğur, and M. Güler, "A theoretical study for the band gap energies of the most common silica polymorphs," *Chinese J. Phys.* **65**, 472–480 (2020).
29. A. Shehata and T. Mohamed, "Method for an accurate measurement of nonlinear refractive index in the case of high-repetition-rate femtosecond laser pulses," *J. Opt. Soc. Am. B* **36**(5), 1246 (2019).
30. M. Falconieri, "Thermo-optical effects in Z-scan measurements using high-repetition-rate lasers," *J. Opt. A: Pure Appl. Opt.* **1**(6), 662–667 (1999).
31. A. Gnoli, L. Razzari, and M. Righini, "Z-scan measurements using high repetition rate lasers: how to manage thermal effects," *Opt. Express* **13**(20), 7976 (2005).
32. G. Rasskazov, A. Ryabtsev, D. Pestov, B. Nie, V. V. Lozovoy, and M. Dantus, "Anomalous laser-induced group velocity dispersion in fused silica," *Opt. Express* **21**(15), 17695 (2013).
33. J. Darginavičius, D. Majus, V. Jukna, N. Garejev, G. Valiulis, A. Couairon, and A. Dubietis, "Ultrabroadband supercontinuum and third-harmonic generation in bulk solids with two optical-cycle carrier-envelope phase-stable pulses at 2 μ m," *Opt. Express* **21**(21), 25210 (2013).
34. A. D. Lad, P. Prem Kiran, G. R. Kumar, and S. Mahamuni, "Three-photon absorption in ZnSe and ZnSe/ZnS quantum dots," *Appl. Phys. Lett.* **90**, 1–4 (2007).
35. R. DeSalvo, A. A. Said, D. J. Hagan, E. W. Van Stryland, and M. Sheik-Bahae, "Infrared to ultraviolet measurements of two-photon absorption and n₂ in wide bandgap solids," *IEEE J. Quantum Electron.* **32**(8), 1324–1333 (1996).
36. A. Dragonmir, J. G. Mcinerney, and D. N. Nikogosyan, "Erratum: Femtosecond measurements of two-photon absorption coefficients at $\lambda = 264$ nm in glasses, crystals, and liquids," *Appl. Opt.* **41**(27), 5655 (2002).
37. A. Karatay, H. G. Yaglıoğlu, A. Elmali, M. Parlak, and H. Karaagac, "Thickness-dependent nonlinear absorption behaviors in polycrystalline ZnSe thin films," *Opt. Commun.* **285**(6), 1471–1475 (2012).
38. B. Derkowska, B. Sahraoui, X. N. Phua, and W. Balab, "Defense technical information center compilation part notice title: nonlinear optical properties in ZnSe crystals nonlinear optical properties in ZnSe crystals," *Proc. SPIE* **4412**, 9–12 (2000).
39. J. H. Lin, Y. J. Chen, H. Y. Lin, and W. F. Hsieh, "Two-photon resonance assisted huge nonlinear refraction and absorption in ZnO thin films," *J. Appl. Phys.* **97**(3), 033526 (2005).
40. X. Wang, J. Qiu, J. Song, J. Xu, Y. Liao, H. Sun, Y. Cheng, and Z. Xu, "Upconversion luminescence and optical power limiting effect based on two- and three-photon absorption processes of ZnO crystal," *Opt. Commun.* **280**(1), 197–201 (2007).